Contributions to Game Theory and Management, XVII, 59–73

Impact of Urban Travel Rates on Epidemic Spread and Basic Reproduction Number

Ma Ke and Elena Gubar

St. Petersburg State University,
Faculty of Applied Mathematics and Control Processes,
7/9, Universitetskaya nab., St. Petersburg, 199034, Russia
E-mail: st097507@student.spbu.ru
E-mail: e.gubar@spbu.ru

Abstract This research incorporates urban transit movement into a Susceptiable -Exposed-Infected-Recovered (SEIR) framework to assess how travel rates influence the transmission of disease among three interconnected urban areas. This model allows us to simulate individual movements across multiple cities and their role in disease transmission, capturing the dynamics of infectious disease spread among three cities. By incorporating symmetric travel rates and uniform exposure assumptions, the model provides insight into how human mobility influences the spread of epidemics and the basic reproduction number (R_0). Our analysis demonstrates that travel rates influence the cross-regional transmission dynamics. Our findings provide important guidance for public health policy, suggesting that the role of travel in disease spread should be addressed, with enhanced international cooperation and coordination for effective outbreak control. These findings underscore the importance of implementing timely and stringent travel restrictions as part of public health measures, especially in the early stages of an epidemic.
Keywords: SEIR Model, Travel Rate, Basic Reproduction Number, Travel Restrictions.

1. Introduction

The rapid spread of infectious diseases in our highly interconnected world constitutes a substantial public health challenge. Urban transportation systems, while essential for facilitating interconnectivity and supporting economic development, inadvertently function as conduits for pathogen dissemination (Qian, 2021). Given the expanding urban populations and the resulting demand for efficient transportation networks, it is crucial to comprehend and mitigate the impact of these systems on disease transmission. To address this, we incorporate the dynamics of urban transportation into the Susceptible-Exposed-Infected-Recovered (SEIR) model, a widely recognized framework in epidemiological modeling (Gubar et al., 2023).

The SEIR model represents a sophisticated stage in the progression of infectious disease modeling and is especially appropriate for examining outbreaks such as COVID-19, characterized by specific incubation periods and subsequent immunity post-recovery (Anastassopoulou et al., 2020). Its efficacy has been substantiated through research on a range of diseases, including influenza (Saito et al., 2013), Ebola (Diaz et al., 2018), and COVID-19 (Yang et al., 2020). Nonetheless, conventional implementations of the SEIR model frequently disregard the complexities inherent in urban environments comprising multiple interconnected regions. This omission can lead to predictions of diminished accuracy and, consequently, less effective policy interventions.

https://doi.org/10.21638/11701/spbu31.2024.06

Our approach involves enhancing the conventional SEIR model by incorporating travel rate parameters to connect three distinct urban centers, thereby improving its applicability to real-world urban settings. This augmented model allows us to simulate individual movements across multiple regions and their role in disease transmission, capturing the dynamics of infectious disease spread among three interconnected cities. By examining varying travel rates, our objective is to identify key factors influencing disease spread, providing a critical basis for targeted intervention strategies. These insights are particularly valuable for decision-making on the implementation of lockdowns during outbreaks to effectively curtail the spread of infections across different urban regions.

The context of our study includes the implementation of travel quarantines and their effects on disease dynamics. Specifically, we examine how travel rates between three cities influence disease transmission, drawing insights into the interplay between urban mobility and the spread of infectious diseases. Our research progresses from the foundational SEIR model, through the incorporation of travel rates connecting three cities, to the development of a novel infectious disease model. We then analyze how variations in travel rates affect the basic reproduction number R_0, highlighting the significant impact of these travel connections on disease dynamics.

By integrating the dynamics of urban transportation into the SEIR model for multiple cities, we provide a more comprehensive understanding of how infectious diseases proliferate in interconnected urban environments. This enhanced model serves as a valuable tool for predicting disease spread and implementing timely measures to curtail disease propagation.

The first part of this article begins with an overview of the fundamental SEIR model for infectious disease dynamics. In the second section, to enhance realism, we extend the basic model by incorporating real-life travel dynamics among three regions, allowing us to better capture cross-regional interactions. In the third section, we introduce a travel rate parameter to quantify and analyze the influence of movement between regions on disease spread. In Section fourth, we employ the next-generation matrix approach to derive a generalized expression for the basic reproduction number R_0, accounting for the effects of interregional travel. Finally, using data from three countries, we investigate how varying travel rates impact the progression of infectious diseases, offering insights into the interplay between mobility and disease transmission.

2. Modeling Disease Spreading with Travel Contagion

2.1. Basic SEIR Model and Specific Components

A generalized SEIR modeling framework was adopted, analogous to that proposed by (Peng et al., 2020), was adopted to facilitate the testing of control interventions. Mathematical models based on dynamical equations often provide insights into epidemic dynamics that are not available from statistical methods alone. Throughout human history, numerous epidemics have emerged, including dengue fever, malaria, influenza, plague, and HIV/AIDS. The development of accurate epidemiological models for these diseases presents a significant challenge. Some researchers adopt a complex network perspective in their analysis of disease transmission, employing this approach for forecasting and modeling purposes (Cantó et al., 2017). To illustrate, in the context of the ongoing pandemic (Prasse et al.,2020)

devised a network-based model that incorporates urban centers and traffic patterns to capture the epidemic dynamics in Hubei province.

Currently, models such as the SIS (van den Driessche et al.,2000), SIR (Cai,2017), and SEIR (Almeida, 2018) are widely used to simulate the spread of infectious diseases. A substantial body of research has demonstrated that these models are an accurate reflection of the dynamics of a range of epidemics. For example, Tang et al. (Tang, B et al., 2020) investigated a generalized SEIR model that incorporates interventions such as quarantine, isolation, and treatment, demonstrating its versatility in addressing real-world scenarios. These frameworks collectively enhance our capacity to predict and control epidemics. Thus in this paper, we try to propose a SEIR model to simulate the process of COVID-19.

The SEIR model, an extension of the SIR model, classifies individuals into four compartments: Susceptible (S), Exposed (E), Infected (I) and Recovered (R).

To begin, we define n_S as the number of individuals in the susceptible group; n_E as the number of individuals in the exposed group; n_I as the number of individuals in the infected group; and n_R as the number of recovered individuals. The total population N is represented as the sum of these compartments: $N = n_S + n_E + n_I + n_R$. At any given time t, the compartments are described in the following proportions: $S(t) = \frac{n_S}{N}$ represents the susceptible population, which includes healthy individuals not yet exposed to the disease. $E(t) = \frac{n_E}{N}$ represents the exposed population, consisting of individuals who have contracted the virus but do not yet show symptoms. $I(t) = \frac{n_I}{N}$ represents the infected population, consisting of individuals exhibiting symptoms of the disease. $R(t) = \frac{n_R}{N}$ represents the recovered population, consisting of individuals who have recovered and are no longer infectious. The sum of these fractions is equal to one, that is, $1 = S(t) + E(t) + I(t) + R(t)$. Additionally, the rates of death and birth are represented by μ.

The transitions between these compartments are governed by a system of differential equations which describe the dynamics of susceptible, infection, exposure, and recovery. These equations encompass the intricacies involved in the transmission of the disease, rendering the SEIR model an effective instrument for epidemiological studies (Lloyd and May, 1996).

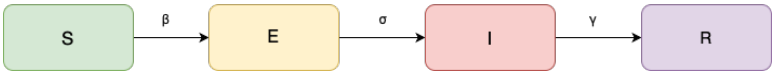

Fig. 1. SEIR model

$$\frac{dS}{dt} = -\beta SI + \mu - S, \tag{1}$$

$$\frac{dE}{dt} = \beta SI - \sigma E - \mu E, \tag{2}$$

$$\frac{dI}{dt} = -\gamma I + \sigma E - \mu I, \tag{3}$$

$$\frac{dR}{dt} = \gamma I - \mu R. \tag{4}$$

The initial conditions for the SEIR model are critical to accurately simulate the progression of an epidemic. The susceptible population (S_0) typically constitutes

the majority of the total population at the start of an epidemic. It is calculated as follows:

$$S_0 = N - E_0 - I_0 - R_{01}, \tag{5}$$

where N is the total population, E_0 represents the initial exposed population, I_0 is the initial infected population and R_{01} is the initial recovered population. These compartments together satisfy the condition $N = S_0 + E_0 + I_0 + R_{01}$, ensuring consistency in population accounting.

In this model, the transmission rate β determines the rate with which susceptible individuals quickly transition to the exposed category after contact with infectious individuals, reflecting the contagiousness of the disease. The progression rate σ specifies how quickly exposed individuals become infectious, acting as a reciprocal of the average incubation period.

2.2. Dynamics of Population Movement Between Cities

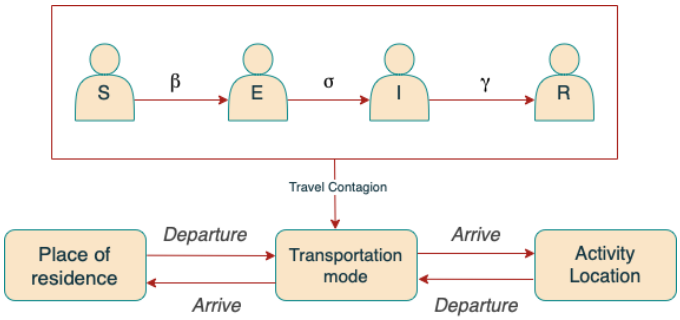

Fig. 2. SEIR Model with Urban Transportation and Travel Contagion Dynamics

In today's interconnected world, the diversity and convenience of transportation options such as airplanes, trains, and ships have significantly enhanced population mobility. However, this increased mobility also presents substantial challenges. The ease with which individuals can move across cities has facilitated the spread of infectious diseases, creating a double-edged sword. As a result, the rapid and widespread transmission of diseases has become a critical concern, particularly in densely populated urban areas.

In our extended SEIR model, we incorporate the dynamics of population movement between three interconnected cities. By modeling intercity movement with travel rate parameters, we can more accurately represent the spread of diseases across urban environments. The movement dynamics are defined by the rates at which individuals travel from one city to another, influencing the transmission and progression of disease in each urban area. The travel rates between cities are denoted as h_{ij}, representing the rate of movement from city i to city j. Including these travel rates allows us to understand the impact of human mobility on the spread of infectious diseases across multiple regions, providing valuable information for targeted intervention strategies.

To make the model more applicable to real-world scenarios, it is necessary to incorporate the impact of travel rates on disease transmission dynamics.

As described by (Sattenspiel and Dietz, 1995) residents of the city i depart from the city at a per capita rate of $g_i \geq 0$ per unit time. The rate of movement from zone i to zone j is denoted as m_{ij}. The departed population then joins the population in travel and will arrive at the activity location with a rate of $\alpha_{\overrightarrow{ij}}$, who again join the population in travel and eventually arrive at home with the rate of $\alpha_{\overleftarrow{ij}}$. In contrast, individuals who have reached the destination city j return to their origin city i at a rate of r_{ij}. The transient population is composed of individuals leaving city i for other cities, as well as those coming into city i from other cities. The product of g_i and m_{ij} represents the rate at which people travel from city i to city j. The travel dynamics between the cities are represented as follows:

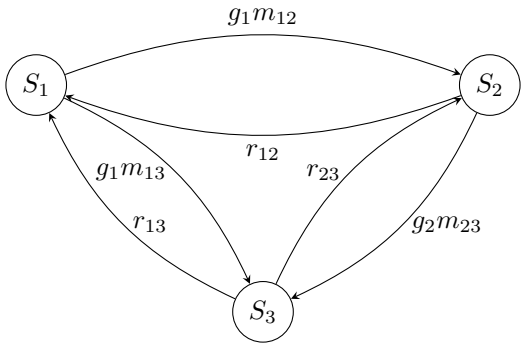

As depicted above, we observe the movement process of susceptible individuals between three cities. This understanding of population movement dynamics is integral to model and predict disease transmission patterns accurately in a three-city SEIR model. The inclusion of intercity travel dynamics in the SEIR model enables us to simulate how infections can spread from one urban area to another, emphasizing the importance of travel restrictions and mobility management during outbreaks.

3. Epidemic Model Equations for Three Cities

The susceptible population (S) denotes individuals who are not yet infected but are likely to be exposed to the virus. For the susceptible population between different cities, we have the following differential equation:

$$\frac{dS_{\overrightarrow{12}}}{dt} = g_1 m_{12} S_1 - \alpha_{\overrightarrow{12}} S_{\overrightarrow{12}} - h_{\overrightarrow{12}}(S,E) - \mu S_{\overrightarrow{12}}, \tag{6}$$

$$\frac{dS_{\overrightarrow{13}}}{dt} = g_1 m_{13} S_1 - \alpha_{\overrightarrow{13}} S_{\overrightarrow{13}} - h_{\overrightarrow{13}}(S,E) - \mu S_{\overrightarrow{13}}, \tag{7}$$

$$\frac{dS_{\overrightarrow{23}}}{dt} = g_2 m_{23} S_2 - \alpha_{\overrightarrow{23}} S_{\overrightarrow{23}} - h_{\overrightarrow{23}}(S,E) - \mu S_{\overrightarrow{23}}, \tag{8}$$

$$\frac{dS_{\overleftarrow{12}}}{dt} = r_{12} S_2 - \alpha_{\overleftarrow{12}} S_{\overrightarrow{21}} - h_{\overleftarrow{12}}(S,E) - \mu S_{\overleftarrow{12}}, \tag{9}$$

$$\frac{dS_{\overleftarrow{13}}}{dt} = r_{13} S_3 - \alpha_{\overleftarrow{13}} S_{\overrightarrow{31}} - h_{\overleftarrow{13}}(S,E) - \mu S_{\overleftarrow{13}}, \tag{10}$$

$$\frac{dS_{\overleftarrow{23}}}{dt} = r_{23} S_3 - \alpha_{\overleftarrow{23}} S_{\overrightarrow{32}} - h_{\overleftarrow{23}}(S,E) - \mu S_{\overleftarrow{23}}, \tag{11}$$

The exposed population (E) represents individuals who have been exposed to the virus but have not yet infected others. For the exposed population across cities, the following differential equation is applicable:

$$\frac{dE_{\overrightarrow{12}}}{dt} = g_1 m_{12} E_1 - \alpha_{\overrightarrow{12}} E_{\overrightarrow{12}} + h_{\overrightarrow{12}}(S,E) - \sigma E_{\overrightarrow{12}} - \mu E_{\overrightarrow{12}}, \tag{12}$$

$$\frac{dE_{\overrightarrow{13}}}{dt} = g_1 m_{13} E_1 - \alpha_{\overrightarrow{13}} E_{\overrightarrow{13}} + h_{\overrightarrow{13}}(S,E) - \sigma E_{\overrightarrow{13}} - \mu E_{\overrightarrow{13}}, \tag{13}$$

$$\frac{dE_{\overrightarrow{23}}}{dt} = g_2 m_{23} E_2 - \alpha_{\overrightarrow{23}} E_{\overrightarrow{23}} + h_{\overrightarrow{23}}(S,E) - \sigma E_{\overrightarrow{23}} - \mu E_{\overrightarrow{23}}, \tag{14}$$

$$\frac{dE_{\overleftarrow{12}}}{dt} = r_{12} E_2 - \alpha_{\overleftarrow{12}} E_{\overrightarrow{21}} + h_{\overleftarrow{12}}(S,E) - \sigma E_{\overleftarrow{12}} - \mu E_{\overleftarrow{12}}, \tag{15}$$

$$\frac{dE_{\overleftarrow{13}}}{dt} = r_{13} E_3 - \alpha_{\overleftarrow{13}} E_{\overrightarrow{31}} + h_{\overleftarrow{13}}(S,E) - \sigma E_{\overleftarrow{13}} - \mu E_{\overleftarrow{13}}, \tag{16}$$

$$\frac{dE_{\overleftarrow{23}}}{dt} = r_{23} E_3 - \alpha_{\overleftarrow{23}} E_{\overrightarrow{32}} + h_{\overleftarrow{23}}(S,E) - \sigma E_{\overleftarrow{23}} - \mu E_{\overleftarrow{23}}, \tag{17}$$

The infected population (I) denotes individuals who are infected and contagious. For the infected population between different cities, we have the following differential equation:

$$\frac{dI_{\overrightarrow{12}}}{dt} = g_1 m_{12} I_1 - \alpha_{\overrightarrow{12}} I_{\overrightarrow{12}} + \sigma E_{\overrightarrow{12}} - \gamma I_{\overrightarrow{12}} - \mu I_{\overrightarrow{12}}, \tag{18}$$

$$\frac{dI_{\overrightarrow{13}}}{dt} = g_1 m_{13} I_1 - \alpha_{\overrightarrow{13}} I_{\overrightarrow{13}} + \sigma E_{\overrightarrow{13}} - \gamma I_{\overrightarrow{13}} - \mu I_{\overrightarrow{13}}, \tag{19}$$

$$\frac{dI_{\overrightarrow{23}}}{dt} = g_2 m_{23} I_2 - \alpha_{\overrightarrow{23}} I_{\overrightarrow{23}} + \sigma E_{\overrightarrow{23}} - \gamma I_{\overrightarrow{23}} - \mu I_{\overrightarrow{23}}, \tag{20}$$

$$\frac{dI_{\overleftarrow{12}}}{dt} = r_{12} I_2 - \alpha_{\overleftarrow{12}} I_{\overrightarrow{21}} + \sigma E_{\overleftarrow{12}} - \gamma I_{\overleftarrow{12}} - \mu I_{\overleftarrow{12}}, \tag{21}$$

$$\frac{dI_{\overleftarrow{13}}}{dt} = r_{13} I_3 - \alpha_{\overleftarrow{13}} I_{\overrightarrow{31}} + \sigma E_{\overleftarrow{13}} - \gamma I_{\overleftarrow{13}} - \mu I_{\overleftarrow{13}}, \tag{22}$$

$$\frac{dI_{\overleftarrow{23}}}{dt} = r_{23} I_3 - \alpha_{\overleftarrow{23}} I_{\overrightarrow{32}} + \sigma E_{\overleftarrow{23}} - \gamma I_{\overleftarrow{23}} - \mu I_{\overleftarrow{23}}, \tag{23}$$

The recovered population (R) denotes the population that has recovered and is immune. For the recovered population across cities, we have the following differential equation:

$$\frac{dR_{\overrightarrow{12}}}{dt} = g_1 m_{12} R_1 - \alpha_{\overrightarrow{12}} R_{\overrightarrow{12}} + \gamma I_{\overrightarrow{12}} - \mu R_{\overrightarrow{12}}, \tag{24}$$

$$\frac{dR_{\overrightarrow{13}}}{dt} = g_1 m_{13} R_1 - \alpha_{\overrightarrow{13}} R_{\overrightarrow{13}} + \gamma I_{\overrightarrow{13}} - \mu R_{\overrightarrow{13}}, \tag{25}$$

$$\frac{dR_{\overrightarrow{23}}}{dt} = g_2 m_{23} R_2 - \alpha_{\overrightarrow{23}} R_{\overrightarrow{23}} + \gamma I_{\overrightarrow{23}} - \mu R_{\overrightarrow{23}}, \tag{26}$$

$$\frac{dR_{\overleftarrow{12}}}{dt} = r_{12} R_2 - \alpha_{\overleftarrow{12}} R_{\overrightarrow{21}} + \gamma I_{\overleftarrow{12}} - \mu R_{\overleftarrow{12}}, \tag{27}$$

$$\frac{dR_{\overleftarrow{13}}}{dt} = r_{13} R_3 - \alpha_{\overleftarrow{13}} R_{\overrightarrow{31}} + \gamma I_{\overleftarrow{13}} - \mu R_{\overleftarrow{13}}, \tag{28}$$

$$\frac{dR_{\overleftarrow{23}}}{dt} = r_{23} R_3 - \alpha_{\overleftarrow{23}} R_{\overrightarrow{32}} + \gamma I_{\overleftarrow{23}} - \mu R_{\overleftarrow{23}}. \tag{29}$$

These equations describe the transmission of infectious diseases between three cities, including travel-based spread and the transition between different compartments.

This transient population is a combination of those leaving city i for other cities $N_{\overrightarrow{ij}}$, and those coming into city i from other cities $N_{\overleftarrow{ij}}$ for all j. In addition, we assume that the exposure levels across cities are relatively uniform or proportional to the population size of each city. Under this assumption, we can approximate:

$$\frac{E_{\overleftarrow{ij}}}{N_{\overleftarrow{ij}}} \approx \frac{E_{\overrightarrow{ij}}}{N_{\overrightarrow{ij}}} \approx \frac{E_{\text{avg}}}{N_{\text{avg}}} = \frac{\sum_{i=1}^{3} E_i}{\sum_{i=1}^{3} N_i}, \tag{30}$$

This approximation allows us to simplify the summation terms into a single average exposure rate across all cities.

For a three-city scenario, we can explicitly write out the transmission dynamics without relying on double summations. With various modes of transportation available, the potential for disease transmission occurs when the exposed population E_{ij} comes into contact with the susceptible population S_{ij} while using a particular mode of transport d at time T. The transmission rate of this interaction is denoted by β_d^T. For example, the travel-based transmission term can be expressed as:

$$h_{\overrightarrow{ij}}(S,E) = \beta_d^T S_{\overrightarrow{ij}} \left(\frac{E_{\overleftarrow{12}}}{N_{\overleftarrow{12}}} + \frac{E_{\overrightarrow{12}}}{N_{\overrightarrow{12}}} + \frac{E_{\overleftarrow{13}}}{N_{\overleftarrow{13}}} + \frac{E_{\overrightarrow{13}}}{N_{\overrightarrow{13}}} + \frac{E_{\overleftarrow{23}}}{N_{\overleftarrow{23}}} + \frac{E_{\overrightarrow{23}}}{N_{\overrightarrow{23}}} \right), \tag{31}$$

This form provides a manageable representation of the transmission dynamics for three interconnected cities.

3.1. Average Transmission Rate Across Cities

If the spread of the disease in cities is relatively similar, we can further simplify by replacing the summation with an average travel-based transmission term:

$$h_{\overrightarrow{ij}}(S,E) \approx \beta_d^T S_{\overrightarrow{ij}} \left(\frac{\sum_{i=1}^{3} \sum_{j=1}^{3} E_{ij}}{\sum_{i=1}^{3} \sum_{j=1}^{3} N_{ij}} \right). \tag{32}$$

This approach effectively reduces the double summation to a single average value, simplifying the equation while preserving the model's overall dynamics.

Considering these factors, our improved SEIR model effectively represents the dynamics of infectious disease transmission both within and between cities. This approach facilitates a more thorough understanding of the role urban transportation plays in epidemic outbreaks and offers essential insights for executing focused public health strategies.

4. Recalculation of Basic Reproduction Number

Definition 1. (Barabási, 2013) The basic reproduction number R_0, represents the average number of susceptible individuals infected by an infected individual during its infectious period in a fully susceptible population.

We employ the next-generation matrix (NGM) methodology as elaborated in (Diekmann et al., 1990; Diekmann and Heesterbeek, 2000). Let F represent the rate of emergence of new infections within compartment i, whereas V indicates the rate at which individuals enter compartment i through alternate mechanisms. To derive the mathematical formulation for R_0 within the framework of the model, we reference the research conducted by (Driessche and Watmough, 2002). In order to simplify the analysis of the three-city model, we introduce two key assumptions: symmetric travel rates and a uniform exposure assumption.

4.1. Simplified Transmission Terms

We assume that the travel rates between cities are symmetric, such that:

$$\alpha_{\overleftarrow{ij}} = \alpha_{\overrightarrow{ij}} \tag{33}$$

This symmetry reduces the number of unique terms in the summation, simplifying the calculation of the total transmission rate across all cities. Using the above assumptions, we can simplify the travel-based transmission term in the three-city model.

For travelers moving from city to city, the transmission term can be expressed as:

$$h_{\overrightarrow{ij}}(S,E) = \beta_d^T S_{\overrightarrow{ij}} \sum_{\text{all travelers}} \frac{E}{N}, \tag{34}$$

Applying the uniform exposure assumption, because there are six categories of travelers in a three-city model, approximate this sum of travelersвЂ™ exposure rates as:

$$\sum_{\text{all travelers}} \frac{E}{N} \approx 6 \times \frac{E_{\text{avg}}}{N_{\text{avg}}}, \tag{35}$$

since there are six categories of travelers in a three-city model (each pair of cities having bidirectional travel).

Thus, the transmission term can be rewritten as:

$$h_{\overrightarrow{ij}}(S,E) = \beta_d^T S_{\overrightarrow{ij}} \times 6 \times \frac{E_{\text{avg}}}{N_{\text{avg}}}, \tag{36}$$

4.2. Constructing the Next-Generation Matrix

The infection term for all exposed individuals is given by:

$$F_i = \beta_d^T S_i \times 6 \times \frac{E_{\text{avg}}}{N_{\text{avg}}}, \tag{37}$$

Transition Term :

For exposed individuals, the transition term is:

$$V_i = (\mu + \sigma + \alpha_i)E_i, \tag{38}$$

Given symmetric travel rates, the net population flow caused by travel cancels out, allowing us to focus solely on disease progression, recovery, and natural mortality in the transition term.

Determining the Jacobian Matrices and the Jacobian of the Infection Term, given that depends linearly on , the elements of the Jacobian matrix are as follows:

$$\frac{\partial F_i}{\partial E_j} = \beta_d^T S_i \times 6 \times \frac{1}{N_{\text{avg}}} \times \frac{\partial E_{\text{avg}}}{\partial E_j}, \tag{39}$$

We have:

$$\frac{\partial E_{\text{avg}}}{\partial E_j} = \frac{1}{3}, \tag{40}$$

Thus, the Jacobian matrix elements are:

$$\frac{\partial F_i}{\partial E_j} = 2\beta_d^T \frac{S_i}{N_{\text{avg}}}, \tag{41}$$

Jacobian of the Transition Term. Given that is solely a function of , the Jacobian matrix is diagonal, and its principal diagonal consists of elements:

$$\frac{\partial V_i}{\partial E_j} = \begin{cases} \mu + \sigma + \alpha_i, & \text{if } i = j \\ 0, & \text{if } i \neq j, \end{cases} \tag{42}$$

The next-generation matrix has elements:

$$K_{ij} = \frac{\partial F_i}{\partial E_j} \times \frac{1}{\mu + \sigma + \alpha_i}, \tag{43}$$

Substituting the previous results:

$$K_{ij} = 2\beta_d^T \frac{S_i}{N_{\text{avg}}} \times \frac{1}{\mu + \sigma + \alpha}. \tag{44}$$

4.3. Calculating the Basic Reproduction Number

In this model, the next generation matrix K exhibits a rank-1 structure, where each row is identical. This implies that transmission between the three cities is uniform, with each exposed individual having the same infection potential regardless of the city they are in. This structure simplifies the analysis, as a rank-1 matrix has only one non-zero eigenvalue, with all other eigenvalues being zero. The assumption of uniform transmission reflects an idealized situation in which the contribution of exposed individuals to the spread of infection is identical across all cities, independent of specific city characteristics.

This simplification significantly facilitates the calculation of the basic reproduction number R_0. Under this condition, the only non-zero eigenvalue of the matrix corresponds to R_0, resulting in $R_0 = 3k$.

Thus, the basic reproduction number is:

$$R_0 = \lambda = 3k = 3 \times 2\beta_d^T \times \frac{1}{\mu + \sigma + \alpha} = \frac{6\beta_d^T}{\mu + \sigma + \alpha}, \tag{45}$$

The basic reproduction number for the three-city model is:

$$R_0 = \frac{6\beta_d^T}{\mu + \sigma + \alpha}. \tag{46}$$

5. Numerical Simulation

The travel policies and behaviors of various countries have had a significant impact on the COVID-19 pandemic. Unlike other nations, Brazil did not initially enforce strict border closures, which likely contributed to the virus's spread. China, conversely, adopted a zero-COVID strategy characterized by swift and strict lockdown alongside extensive testing to suppress transmission (Pequeno et al., 2020). This method was temporarily successful but necessitated substantial social and resource commitment. In Algeria, deficiencies in public health resources and infrastructure (Bentout et al., 2020) could have hindered its ability to effectively manage borders and contain disease spread, compared to other countries.

Table 1. Epidemiological parameters for different regions: Brazil, China and Algeria

Parameter	**Brazil**	**China**	**Algeria**
N_i	45,919,049	9,785,388	1,977,663
β	0.6043	0.4689	0.41
σ	0.2	0.28	0.2
γ	0.1508	0.154	0.1
μ	0.0006	0.0001	0.0001
	(Paul et al., 2021) (Rocha Filho et al., 2021)	(Pang, et al., 2020)	(Bentout et al., 2020)

To perform numerical simulations using the SEIR model, we define the initial conditions for each region based on population data and assumptions regarding the initial states of the epidemic.

The SEIR model consists of four compartments: Susceptible (S), Exposed (E), Infected (I), and Recovered (R). The initial numbers of Exposed (E_0), Infected (I_0), and Recovered (R_0) individuals are determined based on assumptions or available data. For the three regions under consideration, the initial states are defined as follows:

$$E_{1,0} = 10,000, \quad I_{1,0} = 5,000, \quad R_{1,0} = 2,000,$$
$$E_{2,0} = 12,000, \quad I_{2,0} = 6,000, \quad R_{2,0} = 3,000,$$
$$E_{3,0} = 9,000, \quad I_{3,0} = 2,000, \quad R_{3,0} = 1,000.$$

The initial numbers of susceptible individuals (S_0) for each region are calculated using the total population (N) and the initial states of the other compartments,

$$S_{1,2,3}(0) = N_{1,2,3} - E_{1,2,3}(0) - I_{1,2,3}(0) - R_{1,2,3}(0)$$

In addition, based on the assumptions in this study, the initial states of populations related to inter-regional travel are set to zero. For instance:

$$S_{12,0} = S_{13,0} = S_{21,0} = S_{23,0} = S_{31,0} = S_{32,0} = 0,$$

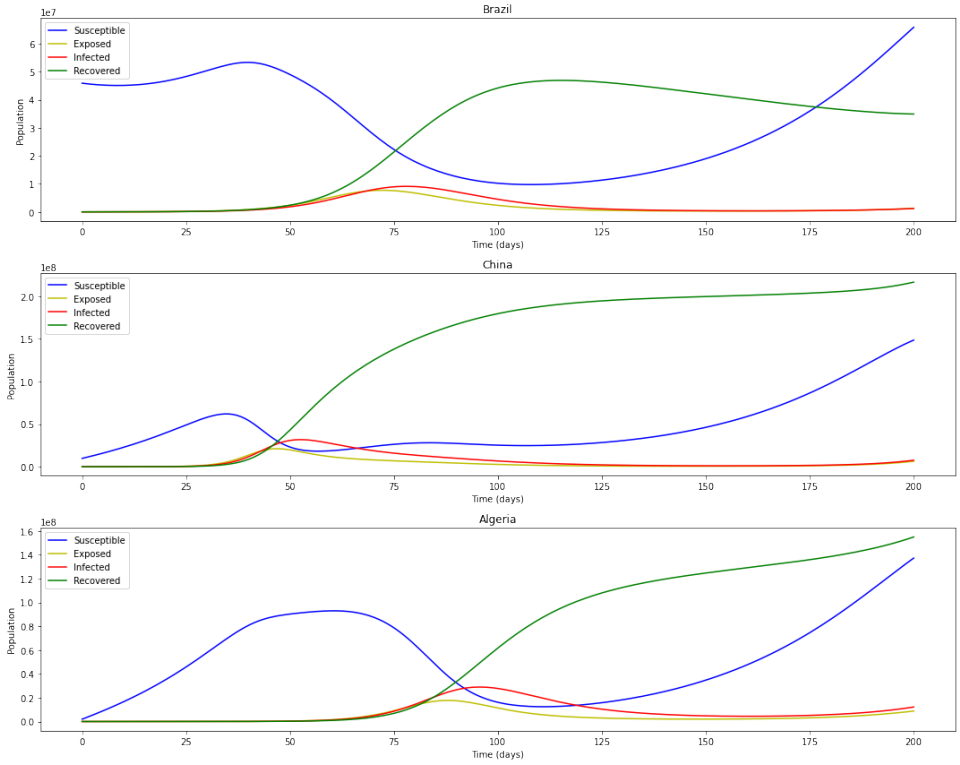

Fig. 3. Dynamics of an SEIR model for two cities over time. A symmetric travel rate was set ($\alpha_{ij} = \alpha = 0.05$). The migration rate was set as $g_i m_{ij} = 0.01$. the disease's progression towards control

The analysis of this figure confirms that our research findings align with the expected outcomes of the model. In Brazil and China, where transmission rates are higher, we observe a rapid decline in the susceptible population and an earlier peak in infections, reflecting faster disease spread. In contrast, Algeria, with a lower transmission rate, shows a slower decline in the susceptible population and a delayed infection peak, consistent with slower epidemic progression. The steady increase in the recovered population in all countries further supports the assumption of the SEIR model that infected individuals eventually transition to immunity. Public health policies should prioritize controlling areas with high transmission rates and strengthen international cooperation to prevent cross-border spread effectively.

6. Impact of Travel Rates on the Basic Reproduction Number R_0

If condition $R_0 < 1$ holds, it is likely that the infection will naturally decline; on the contrary, if $R_0 > 1$, it is expected that the infection will continue to spread and persist within the population. A higher value of R_0 implies a faster spread of the infection. Given that China's value β is relatively high due to data from the early outbreak stage, averaging β values from various sources may not yield a representative value for β_d^T. Instead, we will adopt a practical approach by referencing relevant literature to estimate a reasonable value. In the absence of specific data, we will use a conservative estimate similar to transmission rates reported in close-contact environments in other studies (Pandey et al., 2020;Rahman, B.et al., 2020), setting β_d^T at 0.2 to reflect these practical considerations.

Our calculations indicated that, under symmetric move rates ($\alpha = 0.05$) and uniform exposure assumptions, the values of R_0 for these countries were as follows:

Table 2. Basic Reproduction Number (R_0) for Brazil, China, and Algeria

Country	$\mathbf{R_0}$
Brazil	$R_0^{Brazil} \approx 4.69$
China	$R_0^{China} \approx 3.64$
Algeria	$R_0^{Algeria} \approx 4.80$

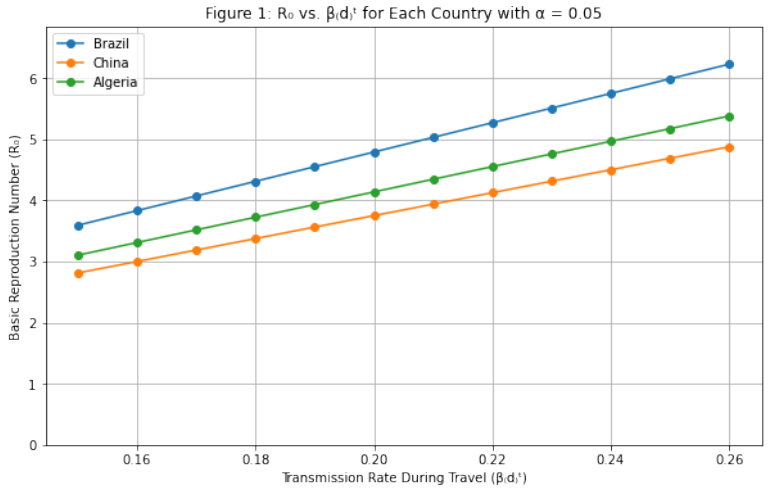

Fig. 4. The relationship between the basic reproduction number R_0 and the transmission rate during travel β_d^T for Brazil, China, and Algeria at a fixed arrival rate $\alpha = 0.05$

These values highlight a higher potential for epidemics in Algeria and Brazil than in China, which may be attributed to their respective transmission rates, natural death rates, and migration or travel behaviors. However, travel rates and interconnectivity also play an essential role in these differences, as travel facilitates

cross-regional transmission, leading to synchronized epidemic peaks and increased infection burdens in interconnected regions.

6.1. Impact of Travel Rates on Epidemic Spread

In countries with high intercity travel rates, such as Brazil, where a high number of confirmed COVID-19 cases appeared early in cities with greater air connectivity, travel has been observed to accelerate the spread of infections across regions (Ribeiro et al., 2020). The role of air travel and the higher population density in Brazilian cities align with host density theories, indicating that densely connected areas with frequent travel are more susceptible to rapid epidemic spread (Poole, 2020). This suggests that cities with high mobility require more targeted interventions to control transmission across the national network.

Similarly, China's rapid and rigorous restrictions on both internal and external travel early in the pandemic, along with strict lockdown measures, were quickly reduced R_0 by limiting population mobility. Despite having a high initial transmission rate ($\beta = 0.78$), China's proactive restrictions curtailed further spread, underscoring the effectiveness of minimizing travel in controlling epidemic transmission.

In Algeria, partial lockdowns and limitations on gatherings had an effect on reducing transmission but were implemented with varying intensity according to region-specific conditions. The relatively high $R_0^{Algeria} \approx 4.80$ despite moderate transmission rates suggests that inconsistent travel restrictions and differing public adherence can impact the effectiveness of these measures. This underlines the need for consistent and well-enforced travel policies to manage transmission between regions.

6.2. Summary of Travel Rate Effects on R_0

Our analysis demonstrates that travel rates significantly impact the basic reproduction number R_0 by influencing the dynamics of transregional transmission. Higher travel rates increase the potential for infection spread between interconnected regions, while restrictive travel policies, as evidenced in China, help to control R_0 by limiting the reach of infections:

- **Increased Travel Rates:** Countries with higher travel rates, like Brazil, face increased infection spread due to the ease with which infections can move between densely populated and connected regions. High travel rates also synchronize epidemic peaks across cities, leading to a more widespread infection burden.
- **Restricted Travel Policies:** Strict border and travel restrictions, as seen in China, help control the spread of infections by reducing R_0. These measures buy time for healthcare system preparation and facilitate a more gradual response, preventing healthcare overload.
- **Importance of Socioeconomic Conditions:** Socioeconomic factors, such as population density and household size, also play a critical role. For example, densely populated areas in Brazil saw a faster spread of COVID-19, while crowded housing conditions and limited sanitation infrastructure in certain regions increased the difficulty of controlling transmission, thus increasing R_0.

7. Conclusions

This study illustrates that travel rates and socioeconomic factors are crucial in determining the dynamics of epidemic spread and the efficacy of interventions.

Higher travel rates contribute to an increase R_0 and a faster spread across interconnected regions, necessitating more robust containment strategies. Countries with higher population density and greater intercity connectivity, like Brazil, can benefit from targeted restrictions in high-mobility areas to reduce transmission risks. In contrast, countries that implemented strict travel limitations, such as China, successfully managed their values R_0 and prevented widespread transmission of epidemics.

These findings underscore the importance of implementing timely and stringent travel restrictions as part of public health measures, especially in the early stages of an epidemic. Furthermore, socioeconomic conditions should be considered when designing these interventions to ensure their effectiveness in different demographic groups. In the context of global interconnectedness, coordinated international health policies are essential to address cross-border transmission and protect vulnerable regions.

References

Almeida, R. (2018). *Analysis of a fractional SEIR model with treatment*. Applied Mathematics Letters, **84**, 56–62.

Anastassopoulou, C., Russo, L., Tsakris, A., Siettos, C. (2020). *Data-based analysis, modelling and forecasting of the COVID-19 outbreak*. PloS one, **15(3)**, e0230405.

Barabási, A. L. (2013). *Network science. Philosophical Transactions of the Royal Society A: Mathematical*, Physical and Engineering Sciences, **371(1987)**, 20120375.

Bentout, S., Chekroun, A., Kuniya, T. (2020). *Parameter estimation and prediction for coronavirus disease outbreak 2019 (COVID-19) in Algeria*. AIMS Public Health, **7**, 306–18.

Biggerstaff, M., Cauchemez, S., Reed, C., Gambhir, M., Finelli, L. (2014). *Estimates of the reproduction number for seasonal, pandemic, and zoonotic influenza: a systematic review of the literature*. BMC infectious diseases, **14(1)**, 1-20.

Cai, Y., Kang, Y., Wang, W. (2017). *A stochastic SIRS epidemic model with nonlinear incidence rate*. Applied Mathematics and Computation, **305**, 221–240.

Cantó, B., Coll, C., Sánchez, E. (2017). *Estimation of parameters in a structured SIR model*. Advances in Difference Equations, 2017, 1–13.

Diaz, P., Constantine, P., Kalmbach, K., Jones, E., Pankavich, S. (2018). *A modified SEIR model for the spread of Ebola in Western Africa and metrics for resource allocation*. Applied mathematics and computation, **324**, 141–155.

Diekmann, O., Heesterbeek, J. A. P. (2000). *Mathematical epidemiology of infectious diseases: model building*, analysis and interpretation **(Vol. 5)**.

Diekmann, O., Heesterbeek, J. A. P., Metz, J. A. (1990). *On the definition and the computation of the basic reproduction ratio R 0 in models for infectious diseases in heterogeneous populations*. Journal of mathematical biology, **28**, 365–382.

Gubar, E., Taynitskiy, V., Fedyanin, D., Petrov, I. (2023). *Quarantine and Vaccination in Hierarchical Epidemic Model*. Mathematics, **11**, 1450.

Gubar, E., Taynitskiy, V., Dahmouni, I. (2023). *The impact of fake news on infection dynamics in Pandemic control: An evolutionary SIR model*. IFAC-PapersOnLine, **56(2)**, 1778-1783.

Lloyd, A. L., May, R. M. (1996). *Spatial heterogeneity in epidemic models*. Journal of theoretical biology, **179(1)**, 1–11.

Pandey, G., Chaudhary, P., Gupta, R., Pal, S. (2020). *SEIR and Regression Model based COVID-19 outbreak predictions in India*. arXiv preprint arXiv:2004.**00958**.

Pang, L., Liu, S., Zhang, X., Tian, T., Zhao, Z. (2020). *Transmission dynamics and control strategies of COVID-19 in Wuhan, China*. Journal of Biological Systems, **28(03)**, 543–560.

Paul, S., Mahata, A., Ghosh, U., Roy, B. (2021). *Study of SEIR epidemic model and scenario analysis of COVID-19 pandemic*. Ecological Genetics and Genomics, **19**, 100087.

Peng, L., Yang, W., Zhang, D., Zhuge, C., Hong, L. (2020). *Epidemic analysis of COVID-19 in China by dynamical modeling*. arXiv preprint arXiv:2002.06563.

Pequeno, P., Mendel, B., Rosa, C., Bosholn, M., Souza, J. L., Baccaro, F., ... and Magnusson, W. (2020). *Air transportation, population density and temperature predict the spread of COVID-19 in Brazil*. PeerJ, 8, e9322.

Poole, L. (2020). *Seasonal influences on the spread of SARS-CoV-2 (COVID19), causality, and forecastabililty* (3-15-2020). Causality, and Forecastabililty **(3-15-2020)**(March 15, 2020).

Prasse, B., Achterberg, M. A., Ma, L., Van Mieghem, P. (2020). *Network-inference-based prediction of the COVID-19 epidemic outbreak in the Chinese province Hubei*. Applied Network Science, **5**, 1–11.

Qian, X., Ukkusuri, S. V. (2021). *Connecting urban transportation systems with the spread of infectious diseases: A Trans-SEIR modeling approach*. Transportation Research Part B: Methodological, **145**, 185–211.

Rahman, B., Sadraddin, E., Porreca, A. (2020). *The basic reproduction number of SARS-CoV-2 in Wuhan is about to die out, how about the rest of the World?*. Reviews in medical virology, **30(4)**, e2111.

Ribeiro, H. V., Sunahara, A. S., Sutton, J., Perc, M., Hanley, Q. S. (2020). *City size and the spreading of COVID-19 in Brazil. PloS one*, **15(9)**, e0239699.

Rocha Filho, T. M., Moret, M. A., Chow, C. C., Phillips, J. C., Cordeiro, A. J. A., Scorza, F. A., ... and Mendes, J. F. F. (2021). *A data-driven model for COVID-19 pandemic-Evolution of the attack rate and prognosis for Brazil*. Chaos, Solitons and Fractals, **152**, 111359.

Saito, M. M., Imoto, S., Yamaguchi, R., Sato, H., Nakada, H., Kami, M., Miyano, S., Higuchi, T. (2013). *Extension and verification of the SEIR model on the 2009 influenza A (H1N1) pandemic in Japan*. Mathematical biosciences, **246(1)**, 47–54.

Sattenspiel, L., Dietz, K. (1995). *A structured epidemic model incorporating geographic mobility among regions*. Mathematical biosciences, **128(1–2)**, 71–91.

Tang, B., Wang, X., Li, Q., Bragazzi, N. L., Tang, S., Xiao, Y., Wu, J. (2020). *Estimation of the transmission risk of the 2019-nCoV and its implication for public health interventions*. Journal of clinical medicine, **9(2)**, 462.

van den Driessche, P., Watmough, J. (2000). *A simple SIS epidemic model with a backward bifurcation*. Journal of Mathematical Biology, **40(6)**, 525–540.

Van den Driessche, P., Watmough, J. (2002). *Reproduction numbers and sub-threshold endemic equilibria for compartmental models of disease transmission*. Mathematical biosciences, **180(1–2)**, 29–48.

Yang, Z., Zeng, Z., Wang, K., Wong, S. S., Liang, W., Zanin, M., ... and He, J. (2020). *Modified SEIR and AI prediction of the epidemics trend of COVID-19 in China under public health interventions*. Journal of thoracic disease, **12(3)**, 165.